

# Disintegration Phenomena Expected During Collision of Comet Shoemaker-Levy 9 with Jupiter

Zdenek Sekanina

In July 1994, periodic comet Shoemaker-Levy 9 is expected to collide with Jupiter. The largest fragments of the comet's original nucleus will be tidally disrupted shortly before they enter the Jovian atmosphere, and all fragments, from large rocks to small grains, will suffer ablation and disintegration as a result of interaction with the atmosphere. Even if atmospheric entry takes place on the planet's far side, secondary phenomena triggered by the terminal explosions of kilometer-sized fragments are likely to be observable from the Earth.

Since its discovery on 24 March 1993 (1), periodic comet Shoemaker-Levy 9 (1993e) has appeared to be an extremely peculiar object. At discovery, its nuclear region consisted of a train of almost perfectly aligned fragments,  $\sim 50$  arc sec long, oriented along a position angle (reckoned from the north through the east) of  $\sim 75^\circ$  and  $255^\circ$ ; the detected number of fragments was 17 or so, depending on the instrumentation used and the observation conditions (2). The train is a boundary of a wide fan of debris that extends to the north and includes tails issuing from the individual fragments at a position angle of  $\sim 285^\circ$  (2). The appearance, which suggests a relatively recent breakup of the comet's original nucleus, has given rise to the object's now commonly used description as a string-of-pearls comet.

The recent improved orbital solutions (3) indicate an extremely close approach to Jupiter on 8 July 1992, when the comet passed only a fraction of the planet's radius above its visible surface. They also suggest that the comet will collide with Jupiter on or around 21 July 1994. Currently, the comet is a Jovian satellite that moves about the planet in a highly eccentric orbit, which is significantly perturbed by the sun and whose current revolution period is about 2.05 years.

The comet almost certainly split during its 1992 close approach to Jupiter because of the planet's tidal forces, possibly assisted by the comet's rotation if rapid enough. This hypothesis is supported by the events observed following an approach to two Jovian radii by periodic comet Brooks 2 in 1886. Subsequent to this comet's discovery in 1889, Barnard (4) detected two major and several short-lived companions to the principal comet. None of the minor fragments were observed more than twice, but the two persisting companions were observed exten-

sively enough to determine that their relative motions were consistent with a primary splitting having taken place at the time of closest approach to Jupiter, on 21 July 1886, which was followed by a secondary breakup about 1.5 years later (5). More recently, the circumstances of the encounter of comet Brooks 2 with Jupiter have been reexamined and constraints on its tensile strength and bulk density have been set (6) by application of the tidal-fission model formulated by Aggarwal and Oberbeck (7).

## Properties of the Fragments

Aggarwal and Oberbeck's model distinguishes between two different modes of tidal fracture. In one of them, fracture begins at the surface of the body and is referred to below as the S mode; in the other, it initiates at the center, hence, the C mode. In the present scenario, the comet's distance  $\Delta_J$  from Jupiter's center in the two modes is expressed in units of the planet's radius  $R_J$

$$\left(\frac{\Delta_J}{R_J}\right)_S = k_S \left(\frac{G \rho_J}{T \rho}\right)^{1/3} \quad (1a)$$

$$\left(\frac{\Delta_J}{R_J}\right)_C = k_C \left(\frac{G \rho_J}{T + \frac{2}{3} G \rho}\right)^{1/3} \quad (1b)$$

where  $\rho_J = 1.33 \text{ g/cm}^3$  and  $\rho$  are the bulk densities of Jupiter and the comet's original nucleus,  $G = \gamma \pi \rho^2 R^2$ , where  $\gamma = 6.67 \times 10^{-8} \text{ dyn cm}^2/\text{g}^2$  is the universal gravitation constant,  $R$  and  $T$  are the effective radius and the tensile strength of the nucleus, and  $k_S$  and  $k_C$  are dimensionless coefficients whose values depend on whether the comet is orbiting Jupiter or collides with the planet.

For orbiting objects, Aggarwal and Oberbeck list three possible fracture sequences, depending, in general, on the

bulk density  $\rho$  and the elasticity. The coefficient of elasticity varies as the square of the product  $\rho R$  and can safely be neglected for cometary nuclei. If the bulk density of P/Shoemaker-Levy 9's original nucleus did not exceed  $\sim 0.66 \text{ g/cm}^3$  and if its breakup on 8 July 1992 occurred at the point of closest approach, when the comet's Jovicentric distance was  $\Delta_J = 116,000 \text{ km} = 1.62 R_J$  according to the most recent (21 July 1993) orbital calculations (3), it is likely that fracture began at the nucleus center and propagated toward the surface, where the breakup was completed. The relevant value of the coefficient  $k_S$  is 0.520, and the ratio of the tensile strength to the bulk density of the comet's original nucleus is, from Eq. 1a

$$T/\rho \approx 92 R^2 \quad (2)$$

where  $T$  is in dynes per square centimeter,  $\rho$  in grams per cubic centimeter, and  $R$  in kilometers. The nuclear radius of the parent comet is unknown, but it can be approximately constrained. A preliminary analysis of observations of the comet with the Hubble Space Telescope (8) indicates that the effective nuclear radius of the brightest fragment is 2.6 km, assuming a geometric albedo of 4% and a phase coefficient of 0.035 mag/degree. This result, corrected for the contamination by the surrounding dust cloud, is obviously a crude lower limit to the nuclear size of the parent comet and yields, from Eq. 2,  $T/\rho \approx 600 \text{ dyn cm/g}$ , an extremely low value. Tighter limits on the mass, dimensions, and tensile strength of the comet's original nucleus result from consideration of the mass distribution of the large fragments. If  $f(M)dM$  is the number of comet fragments with masses between  $M$  and  $M + dM$  and if the  $N$  observed fragments have masses  $M_1 > M_2 > \dots > M_N$ , then

$$N = \int_{M_N}^{M_1} f(M) dM$$

$$M_{\text{total}} = \int_{M_N}^{M_1} M f(M) dM \quad (3)$$

Approximating  $f(M)dM \propto M^{-\alpha}dM$ , where  $\alpha$  introduce a constant mass index  $\alpha$ , and taking, for example,  $N = 17$  (2), one finds

The author is at the Jet Propulsion Laboratory, California Institute of Technology, Pasadena, CA 91109.

$$\frac{M_{\text{total}}}{M_1} = 17 \frac{\alpha - 1}{\alpha - 2} \frac{\mathfrak{R}^{\alpha-2} - 1}{\mathfrak{R}^{\alpha-1} - 1} \text{ for } \alpha \neq 1, 2$$

$$= 17 \frac{\ln \mathfrak{R}}{\mathfrak{R} - 1} \text{ for } \alpha = 2 \quad (4)$$

where  $\mathfrak{R} = M_1/M_{17} > 1$  is the mass ratio of the most and the least massive fragments. The ratio  $M_{\text{total}}/M_1$  can be equivalently expressed as a ratio of the effective nuclear radii,  $R/R_1$ , of the original nucleus and the most massive fragment. Table 1 lists this ratio, as well as the ratio between the tensile strength and the bulk density of the comet's original nucleus, for several combinations of the assumed values of the mass index  $\alpha$  and the mass ratio  $\mathfrak{R}$ . The results depend insignificantly on  $\alpha$  and only moderately on  $\mathfrak{R}$ . Because  $R > R_1$ , large values of  $\alpha$  and  $\mathfrak{R}$  are unacceptable, as indicated in Table 1 by the dots.

The ratio of  $T/\rho$  for the parent comet is thus likely to be  $\sim 1000$  to  $3000$  dyn cm/g. At an assumed bulk density of  $0.2$  to  $0.5$  g/cm<sup>3</sup>, this yields  $T \approx 200$  to  $1500$  dyn/cm<sup>2</sup>, which implies that the comet's nucleus was a very poorly cemented object with hardly any structural cohesion. These estimates of the tensile strength  $T$  can also be used to address the question of the role of the Jovian tidal forces at the time of the collision in July 1994. Again, fracture should proceed in the C mode, and the breakup will be completed at the surface. From Eq. 1a, with  $k_S = 0.595$ , one has for the critical radius of a fragment that will not break up before entering the Jovian atmosphere

$$R_{\text{crit}} = 0.0413 \sqrt{T/\rho}, \quad (5)$$

where  $R_{\text{crit}}$  is in kilometers and  $T/\rho$  in dyne-centimeters per gram. Using the above estimates for  $T/\rho$ , one finds a critical radius of  $R_{\text{crit}} \approx 1.3$  to  $2.3$  km, slightly smaller than the quoted estimate for the brightest fragment. It therefore appears that only a few of the largest fragments are likely to break up before they reach the Jovian atmosphere. The corresponding critical nucleus mass is on the order of  $0.2 \times 10^{16}$  to  $2.5 \times 10^{16}$  g. Less massive fragments are expected to enter the atmosphere unbroken. However, Eq. 1b, with  $k_C = 1.039$  in this case, indicates that by the time of the atmospheric entry, cracks will have developed in the interior of fragments whose radii are as small as  $0.6$  to  $1.1$  km and whose masses are as low as  $0.2 \times 10^{15}$  to  $3 \times 10^{15}$  g. At this point, all the fragments and debris will become subjected to aerodynamic pressure effects of the Jovian atmosphere.

### Impact with Jupiter

The motion of a comet or its fragment through the Jovian atmosphere is a variation of the classical problem of meteor physics, as long as the object's material properties dur-

ing its atmospheric flight are determined primarily by its refractory, rather than volatile, constituent. This assumption is at least qualitatively justified by the failure to detect an OH emission in a spectrum taken with the Hubble Space Telescope (8). The basic issues involved are, in that case, (i) a deceleration caused by atmospheric drag, which counters an acceleration attributable to the planet's gravitational attraction, and (ii) a progressive mass ablation caused by heating from the atmospheric shock front. The general formulas used for the rates of change in the projectile's velocity  $V$  and its residual mass  $m$  are

$$\dot{V} = -\frac{F}{m} P + \frac{\gamma M_J}{\Delta_J^2} \cos Z$$

$$\dot{m} = -\sigma F V P \quad (6)$$

where  $M_J$  is Jupiter's mass,  $Z$  is the local zenith angle of the projectile's trajectory,  $F$  is its instantaneous frontal area,  $\sigma$  is its ablation coefficient (which is approximately constant throughout the atmospheric flight and whose dimension is that of a reciprocal square of the velocity), and  $P$  is the local aerodynamic pressure exerted on the object

$$P = \Gamma \rho_{\text{atm}} V^2, \quad (7)$$

where  $\Gamma = 1/2 C_D$  is a drag coefficient and  $\rho_{\text{atm}}$  is the local atmospheric density. The density profile of the Jovian atmosphere was taken from Orton's model (9), which was generated for the Galileo Project. The nominal zero height was taken to refer to an equatorial radius of  $71,495$  km to fit the  $100$ -mbar isobaric level, which was determined from the Voyager measurements to correspond to  $71,541$  km from the planet's center (10) and, in Orton's model, corresponds to a height of  $46$  km. Neglected is a very slight bending of the atmospheric trajectory that is caused by the  $\sin Z$  component of the gravitational acceleration (normal to the projectile's direction of motion).

The results presented below refer to two kinds of objects interacting with the Jovian atmosphere:

1) A rigid spherical impactor, whose surface ablates uniformly, which is subjected to no deformations and experiences no

fragmentation episodes during its atmospheric flight. With these somewhat unrealistic, yet often used, assumptions, the object's shape does not change along the trajectory; therefore, it is customary to introduce a shape factor  $A$ , whose value for spheres is  $(9\pi/16)^{1/3} \approx 1.2$ , and to write for the projectile's instantaneous frontal area  $F = A(m/\rho)^{2/3}$ . Since  $A$  and  $\rho$  are assumed to be constant,  $\dot{F} < 0$  because  $\dot{m} < 0$ . The expression for the drag-driven deceleration then becomes

$$\dot{V}_{\text{drag}} = -\Gamma A \rho_{\text{atm}} m^{-2/3} V^2 \quad (8)$$

The ablation equation can be integrated in close form if the gravitational term  $\dot{V}_{\text{grav}}$  in the deceleration equation (Eq. 6) is neglected. I prefer to retain it in the present calculations and integrate both the deceleration equation and the ablation equation numerically.

2) A cylindrical impactor, whose initial length is equal to its diameter, which penetrates the atmosphere along its axis of symmetry and is subjected to deformations that satisfy the condition (11)

$$\dot{R} = \frac{P}{\rho R} \quad (9)$$

where  $\rho$  is again the object's bulk density and  $R$  its time-dependent radius. This condition is applicable when the aerodynamic pressure (Eq. 7) exceeds, or is equal to, the material strength  $T_c$  of the projectile. When  $P < T_c$ , there are no deformations and  $\dot{R} = 0$ . The preatmospheric radius  $R_\infty$  of the cylinder is related to its preatmospheric mass  $m_\infty = M$  by  $R_\infty = (m_\infty/2\pi\rho)^{1/3}$ , and the frontal area  $F = \pi R_\infty^2$  remains constant as long as  $P \leq T_c$ . Because  $\dot{F} > 0$  while  $\dot{m} < 0$  at higher aerodynamic pressures, the ablation of this nonrigid cylindrical model projectile proceeds at the expense of its length.

The diverse temporal variations in the frontal area represent the fundamental difference between the two models. Even though the nonrigid cylinder is highly idealized and may have to be replaced by a more sophisticated model in the future, a side-by-side comparison of the two models illustrates the effects of a projectile's expanding cross-sectional area

**Table 1.** Ratio of nucleus radii of the parent comet and the most massive fragment ( $R/R_1$ ) and the ratio of the tensile strength to the bulk density ( $T/\rho$ ) for the parent comet.

Mass ratio $\mathfrak{R}$	Ratio of nucleus radii, $R/R_1$			Ratio of strength to density, $T/\rho$ (dyn cm/g)		
	$\alpha = 1.5$	$\alpha = 2.0$	$\alpha = 2.5$	$\alpha = 1.5$	$\alpha = 2.0$	$\alpha = 2.5$
2	2.29	2.28	2.26	3520	3490	3430
5	1.97	1.90	1.84	2600	2420	2270
10	1.75	1.63	1.53	2050	1780	1570
20	1.56	1.39	1.26	1630	1300	1060
50	1.34	1.19	...	1200	950	...
100	1.19	...	...	950	...	...

on the height of the terminal point (at which the object disintegrates completely), on the peak aerodynamic pressure that is tolerated by the projectile before its disintegration, and on the rate of energy dissipation attributable to its ablation and deceleration. Neither of the two models includes gross-fragmentation events, to which fireballs in the Earth's atmosphere are known to be susceptible often at dynamic pressures that are significantly lower than those expected from laboratory tensile and compressive strength tests.

The most recent orbital results [for example, (3)] indicate with virtual certainty that all major fragments of P/Shoemaker-Levy 9 are heading for a collision with Jupiter in the sense that their trajectories are projected to cross, in late July 1994, the planet's "surface," as conventionally defined. The orbital elements calculated by Yeomans and Chodas in July 1993 suggest the most probable distance at the time of closest approach to be 37,000 km, or 0.52  $R_J$ , from the planet's center. Because forthcoming astrometric observations will unquestionably lead to further refinements of the orbit in the near future, it seems prudent to investigate the effects of the minimum distance  $(\Delta_J)_{\min}$  on the models. The other variable whose wide range has been considered is the preatmospheric mass,  $m_\infty$ , of the fragments. The upper limit has been set at  $10^{18}$  g to allow for a safe margin in accounting for the largest possible bodies that could resist tidal fracture. Because of a vast amount of dust accompanying the major fragments, it was deemed appropriate to extend the mass range down to boulders, pebbles, and grains; the lower limit was thus set rather arbitrarily at 1 g.

To keep the amount of calculations tractable, certain parameters were not varied at all in most runs. The bulk density  $\rho$  and the ablation coefficient were taken to be equal to their characteristic values for the "soft" cometary fireballs, of class IIIb (12):  $\rho =$

$0.2 \text{ g/cm}^3$  and  $\sigma = 0.20 \text{ s}^2/\text{km}^2$ . For deforming projectiles, a material strength of  $T_c = 10^4 \text{ dyn/cm}^2 = 10^{-2} \text{ bar}$  was assumed, about one order of magnitude higher than the tensile strength estimated above and near the lower limit to a critical dynamic pressure at which the highly fragile Giacobinid fireballs are known to begin to flare up and disintegrate [see, for example, (13)]. The drag coefficients were taken to have the usual values  $\Gamma_{\text{sphere}} = 0.60$  and  $\Gamma_{\text{cylinder}} = 0.85$ , and the impactors were assumed to approach with the parabolic velocity.

The integrations were initiated at an altitude of 1000 km above the 1-bar pressure level, where the pressure according to Orton's equatorial model is about 23 pbar and where both the ablation rate and the rate of deceleration were found to be extremely minute even for the least massive projectiles considered. In fact, it was found that the gravitational acceleration  $\dot{V}_{\text{grav}}$  was invariably much greater in magnitude than the drag deceleration  $\dot{V}_{\text{drag}}$  at these high altitudes. To account properly for the amount of the projectile's energy dissipated during a very short interval of time  $dt$ , the change in the kinetic energy in the atmosphere,  $dE_{\text{atm}}(t) = 1/2(m + \dot{m} dt)[V + (\dot{V}_{\text{drag}} + \dot{V}_{\text{grav}})dt]^2 - 1/2mV^2$ , was corrected for an equivalent change in the energy in the absence of an atmosphere,  $dE_{\text{vacuum}}(t) = 1/2m(V + \dot{V}_{\text{grav}} dt)^2 - 1/2mV^2$ . The net dissipated energy,  $dE$ , was calculated with the terms of the higher powers of  $dt$  retained; although, in order to illustrate the effect, one may neglect these and find

$$dE = -(m\dot{V}_{\text{drag}} + 1/2\dot{m}V)V dt \quad (10)$$

Because  $\dot{V}_{\text{drag}} < 0$  and  $\dot{m} < 0$ , one finds that  $dE > 0$ . At first sight, the dissipated energy appears to be independent of  $\dot{V}_{\text{grav}}$ , which is always positive on the way in but becomes negative for the fragments that have survived their fiery encounter with the atmosphere past the point of closest approach. In

fact, of course,  $\dot{V}_{\text{grav}}$  is involved implicitly in the values of  $V$ . In practice, however, the integrated effect of the  $\dot{V}_{\text{grav}}$  term has never been found to exceed 0.4 km/s in the considered scenarios, which is insignificant enough so that the cumulative energy  $E$  dissipated by any completely ablated object (in megatons of TNT) can be described in terms of its preatmospheric mass  $m_\infty$  (in grams)

$$E = 4.2 \times 10^{-10} m_\infty \quad (11)$$

The results are presented according to the physical model (rigid sphere versus nonrigid cylinder) and trajectory type (deep penetration versus grazing encounter). The major differences in the physical characteristics of the two sets of model projectiles are apparent from comparison of Tables 2 and 3. As expected, for a trajectory of the same minimum distance from the planet's center and for the same initial mass of the projectile, rigid objects penetrate deeper into the atmosphere than deformable ones. The differences in the terminal height vary from less than 30 km for a mass of  $10^{16}$  g to more than 90 km for  $10^6$  g. In terms of the atmospheric pressure at the terminal point, the differences range from a factor of  $\sim 3$  up to a factor of  $\sim 25$ . The peak dynamic pressures sustained show similar, but somewhat smaller, differences. The peak relative energy dissipation rates are generally higher for the nonrigid objects and reach sharply higher values for low masses, except when the peak dynamic pressure fails to reach the material strength. The rates greater than  $1 \text{ s}^{-1}$ , common for nonrigid objects (Table 2), imply that they cannot be sustained for longer than a small fraction of a second and that they therefore signify events that can only be described as explosions. The propensity for this behavior is far less apparent among the rigid objects (Table 3). Finally, for the given kind and mass of the object, the terminal height, the peak aerodynamic

**Table 2.** Height and pressure at the terminal point in the Jovian atmosphere and the peak aerodynamic pressure and relative energy dissipation rate for nonrigid cometary objects of a variety of masses that enter the

Jovian atmosphere along deep-penetration trajectories [ $(\Delta_J)_{\min} < R_J$ ] with a parabolic velocity (59.12 km/s at a height of 1000 km and atmospheric pressure of  $\sim 23$  pbar).

Preatmospheric mass $m_\infty$ (g)	Trajectory's minimum distance from Jupiter's center, $(\Delta_J)_{\min} = 0 R_J$				Trajectory's minimum distance from Jupiter's center, $(\Delta_J)_{\min} = 0.5 R_J$				Trajectory's minimum distance from Jupiter's center, $(\Delta_J)_{\min} = 0.9 R_J$			
	$H_{\text{terminal}}$ (km)	$p_{\text{terminal}}$ (bar)	$P_{\text{peak}}$ (bar)	$(\dot{E}/E)_{\text{peak}}$ ( $\text{s}^{-1}$ )	$H_{\text{terminal}}$ (km)	$p_{\text{terminal}}$ (bar)	$P_{\text{peak}}$ (bar)	$(\dot{E}/E)_{\text{peak}}$ ( $\text{s}^{-1}$ )	$H_{\text{terminal}}$ (km)	$p_{\text{terminal}}$ (bar)	$P_{\text{peak}}$ (bar)	$(\dot{E}/E)_{\text{peak}}$ ( $\text{s}^{-1}$ )
$10^{18}$	-10	1.4	6100	1.9	-6	1.2	5600	1.8	11	0.62	3400	1.1
$10^{16}$	26	0.29	2000	3.0	29	0.25	1700	2.7	42	0.12	900	1.5
$10^{14}$	56	0.059	390	3.3	59	0.051	330	2.9	75	0.024	140	1.5
$10^{12}$	95	0.0090	49	3.2	99	0.0074	41	2.9	122	0.0031	15	1.5
$10^{10}$	148	0.0011	5.5	3.6	154	0.00090	4.5	3.2	179	0.00035	1.7	1.7
$10^8$	207	0.00013	0.62	4.3	212	0.00011	0.50	3.7	238	0.000044	0.20	2.1
$10^6$	263	0.000018	0.076	5.5	268	0.000016	0.064	5.0	287	0.0000079	0.032	3.2
$10^4$	302	0.0000047	0.019	10.8	305	0.0000043	0.018	10.2	313	0.0000032	0.014	8.1
$10^2$	318	0.0000027	0.012	28.6	318	0.0000027	0.011	26.4	321	0.0000024	0.010	10.9
1	337	0.0000014	0.0060	1.9	342	0.0000012	0.0052	1.6	362	0.00000061	0.0026	0.8

pressure, and the peak energy dissipation rate are almost independent of the trajectory's minimum distance until this distance is comparable with the radius  $R_J$ .

Tables 2 and 4 illustrate the major differences in the behavior of projectiles approaching along grazing trajectories in comparison with those moving in deep-penetration trajectories. The tabulated results refer to nonrigid objects, but differences of this magnitude apply generally. One also notices the extreme sensitivity of the results on the minimum distance, unlike for most of the deep-penetration trajectories. The values of the atmospheric pressure at the terminal height, the peak dynamic pressure, and the energy dissipation rate are all substantially lower in grazing trajectories (Table 4) compared with those for penetration trajectories (Table 2). An interesting qualitative difference is that massive projectiles can survive their flight through the Jovian atmosphere; Table 4 shows two such cases, and in both, the total exerted deceleration is virtually negligible (14). This table also lists a case in which the projectile survived the flight through the point of minimum distance but disintegrated on the way out of the atmo-

sphere. Although no data are presented for the rigid objects in grazing trajectories, their models have been calculated to the same extent as for the nonrigid projectiles, and the differences between the two kinds of object are again very clearly apparent. For example, the masses that survive the flight in the trajectory with a minimum height of 200 km are found to extend from  $10^{16}$  g upward for nonrigid projectiles, but from  $10^{12}$  g upward for rigid projectiles.

Predictions for 1994

Considering the current scenario for the collision in July 1994, where  $(\Delta_J)_{\min} = 0.52 R_J$ , the most likely impact circumstances are described in the middle columns of Table 2. The most spectacular phenomena will be triggered by impacts of the major fragments of an estimated mass of  $\sim 10^{16}$  g. The fragments apparently will be capable of penetrating the atmosphere to considerable depths, almost to the pressure level of 1 bar, where they will experience aerodynamic pressures of  $\sim 10^3$  bar, some five orders of magnitude higher than their estimated material strength. The calculations for nonrigid pro-

jectiles predict that the rates of energy and mass dissipation will peak very sharply at the end of the trajectory (Fig. 1). During this terminal explosion, the projectile's residual mass, still a substantial fraction of the initial mass, will be instantly shattered by the strong shock wave into a cloud of particulates, only some of which will vaporize before they can expand.

The properties of a shock wave propagating from a point energy source into an exponential atmosphere have been investigated theoretically (15). The shock envelope expands preferentially upward and eventually opens up and "leaks" the energy (and microscopic ejecta) into outer space. The result in the case of the collision of P/Shoemaker-Levy 9 with Jupiter is very difficult to predict because of several complicating factors, such as recondensation of the vaporized material, as well as Jupiter's gravity, rapid rotation, and atmospheric circulation. In any case, sunlight will be scattered by the dust that will end up temporarily suspended in the atmosphere and perhaps even ejected into ballistic trajectories in the immediate proximity of the planet, and the resulting optical effects may be observable from the Earth. Indeed, if a fraction  $f$  of the

Table 3. Same parameters and conditions as Table 2 for rigid spherical cometary objects.

Preatmospheric mass $m_\infty$ (g)	Trajectory's minimum distance from Jupiter's center, $(\Delta_J)_{\min} = 0 R_J$				Trajectory's minimum distance from Jupiter's center, $(\Delta_J)_{\min} = 0.5 R_J$				Trajectory's minimum distance from Jupiter's center, $(\Delta_J)_{\min} = 0.9 R_J$			
	$H_{\text{terminal}}$ (km)	$p_{\text{terminal}}$ (bar)	$P_{\text{peak}}$ (bar)	$(\dot{E}/E)_{\text{peak}}$ (s <sup>-1</sup> )	$H_{\text{terminal}}$ (km)	$p_{\text{terminal}}$ (bar)	$P_{\text{peak}}$ (bar)	$(\dot{E}/E)_{\text{peak}}$ (s <sup>-1</sup> )	$H_{\text{terminal}}$ (km)	$p_{\text{terminal}}$ (bar)	$P_{\text{peak}}$ (bar)	$(\dot{E}/E)_{\text{peak}}$ (s <sup>-1</sup> )
$10^{18}$	-54	4.6	9400	0.90	-48	4.0	8500	0.79	-22	2.0	5400	0.51
$10^{16}$	-1	1.0	3400	1.32	3	0.89	3100	1.19	19	0.44	1900	0.62
$10^{14}$	32	0.21	1000	1.37	35	0.18	900	1.21	47	0.093	450	0.59
$10^{12}$	61	0.048	210	1.25	63	0.042	180	1.07	77	0.022	87	0.46
$10^{10}$	93	0.010	37	0.99	96	0.0085	32	0.87	113	0.0044	16	0.43
$10^8$	131	0.0022	7.1	0.98	135	0.0019	6.1	0.87	153	0.00091	3.1	0.44
$10^6$	172	0.00044	1.5	1.00	176	0.00038	1.3	0.87	194	0.00020	0.67	0.44
$10^4$	214	0.00010	0.33	0.99	218	0.000090	0.28	0.79	236	0.000047	0.14	0.39
$10^2$	256	0.000024	0.068	0.86	260	0.000020	0.058	0.76	279	0.000010	0.029	0.39
1	301	0.0000049	0.014	0.87	305	0.0000042	0.012	0.76	326	0.0000021	0.0060	0.38

Table 4. Same parameters and conditions as Table 2 for nonrigid cometary objects that enter the Jovian atmosphere along grazing trajectories [ $(\Delta_J)_{\min} \approx R_J$ ].

Preatmospheric mass $m_\infty$ (g)	Trajectory's minimum distance from Jupiter's center, $(\Delta_J)_{\min} = 0.99 R_J$				Trajectory's minimum distance from Jupiter's center, $(\Delta_J)_{\min} = 1 R_J$				Trajectory's minimum distance from Jupiter's center, $(\Delta_J)_{\min} = 1.0028 R_J^*$			
	$H_{\text{terminal}}$ (km)	$p_{\text{terminal}}$ (bar)	$P_{\text{peak}}$ (bar)	$(\dot{E}/E)_{\text{peak}}$ (s <sup>-1</sup> )	$H_{\text{terminal}}$ (km)	$p_{\text{terminal}}$ (bar)	$P_{\text{peak}}$ (bar)	$(\dot{E}/E)_{\text{peak}}$ (s <sup>-1</sup> )	$H_{\text{terminal}}$ (km)	$p_{\text{terminal}}$ (bar)	$P_{\text{peak}}$ (bar)	$(\dot{E}/E)_{\text{peak}}$ (s <sup>-1</sup> )
$10^{18}$	34	0.19	1400	0.47	56	0.059	390	0.15	... †	.....	0.81 ‡	0.017 §
$10^{16}$	64	0.040	250	0.50	89	0.012	67	0.18	...	.....	0.81 ‡	0.016 ¶
$10^{14}$	106	0.0058	31	0.51	134	0.0019	9.4	0.23	210 #	0.00012	0.81 ‡	0.037
$10^{12}$	160	0.00071	3.6	0.60	187	0.00026	1.3	0.32	219	0.000087	0.40	0.15
$10^{10}$	218	0.000090	0.42	0.72	241	0.000039	0.17	0.42	262	0.000019	0.080	0.26
$10^8$	271	0.000014	0.056	0.99	288	0.0000077	0.031	0.68	299	0.0000052	0.021	0.54
$10^6$	306	0.0000041	0.017	2.13	313	0.0000032	0.014	1.76	316	0.0000028	0.012	1.51
$10^4$	319	0.0000026	0.011	5.36	321	0.0000024	0.010	2.57	327	0.0000020	0.0085	0.12
$10^2$	344	0.0000011	0.0048	0.32	360	0.00000065	0.0028	0.19	370	0.00000048	0.0020	0.13
1	392	0.00000026	0.00096	0.30	408	0.00000016	0.00056	0.18	418	0.00000012	0.00040	0.13

\*Corresponds to a height of 200 km. †Object escapes into space with 98.5% of its mass surviving and a velocity of 59.12 km/s at a height of 1000 km. ‡At point of closest approach. §Cumulative dissipated energy is  $E = 6.5 \times 10^{12}$  tons of TNT or 1.5% of the object's initial kinetic energy. ||Escapes with 91.7% of its mass

and a velocity of 59.11 km/s at a height of 1000 km. ¶Cumulative dissipated energy is  $E = 0.35 \times 10^{12}$  tons of TNT or 8.3% of the object's initial kinetic energy. #Projectile survives its flight through the point of minimum distance but disintegrates on the way out of the atmosphere.

total mass  $M_{\text{total}}$  of the major fragments disintegrates into a large number of microscopic particles, each of a mass  $\mu$  and bulk density  $\rho_{\mu}$ , the total projected cross-sectional area of the debris can be estimated at  $\sim 1.2fM_{\text{total}}\mu^{-1/3}\rho_{\mu}^{-2/3}$ , which, with conservative input estimates ( $M_{\text{total}} \approx 10^{17}$  g,  $\mu \approx 10^{-12}$  g, and  $\rho_{\mu} \approx 1$  g/cm<sup>3</sup>), yields a cross-sectional area of  $1.5 \times 10^9$  km<sup>2</sup>, equal to that of Jupiter when  $f \approx 0.1$ . Hence, it is not out of the question that a temporary brightening of the planet attributable to the presence of the comet's dust will be visible from the Earth.

On the other hand, the comet's fragments that enter the Jovian atmosphere with initial masses  $\ll 10^{16}$  g will disintegrate in a less harsh environment of higher altitudes and will generate less powerful explosions. Projectiles in the centimeter-to-submeter size range are expected to ablate away completely at altitudes of 300 to 400 km, having been exposed to aerodynamic pressures that do, if at all, only marginally exceed the estimated material strength. The indication therefore is that the atmospheric levels with a pressure of hundreds of millibars will be affected most severely, but the contamination by cometary dust is likely to involve a considerably greater volume of the atmosphere.

Besides the large amounts of cometary dust particles temporarily suspended in the Jovian atmosphere and hopefully observable for some period of time because of their scattering of sunlight, additional visual effects are also likely to be detected. Most of the brightest fireballs striking the Earth's atmosphere display light curves that bear a strong resemblance to the derived curves in Fig. 1 [see, for example, (16)]. Indeed,

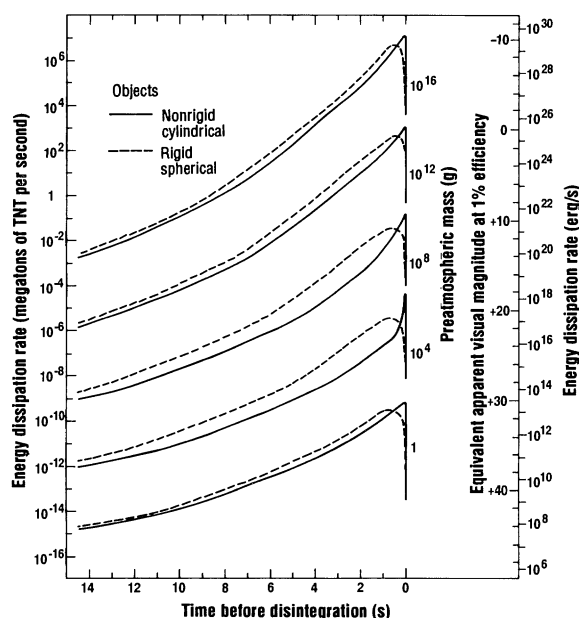
because the second term on the right side of Eq. 10 is always found in the scenarios considered here to dominate by orders of magnitude (probably because of the high velocities involved and the high ablation coefficient assumed), the energy dissipation curves are essentially identical with the ablation curves. However, an ablation curve can only be transformed into a light curve when a complicated conversion function, called a luminous efficiency, is known. Its determination for fireballs penetrating the Earth's atmosphere has been a subject of a large number of investigations in the past 60 years; even so, different physical models predict luminous efficiencies that differ from one another by orders of magnitude [see (17) for an example]. In general, the luminous efficiency depends on the fireball's composition and on its velocity and mass and the local atmospheric density, which determine the flow regime (18). The average values that are found in the literature range from less than 0.1% to more than 10% of the projectile's total kinetic energy available. The luminous efficiency has a tendency to increase with velocity for slow meteors and fireballs but to decrease, perhaps asymptotically, at high velocities, such as those to be experienced by the fragments of P/Shoemaker-Levy 9 in July 1994. Finally, of course, the luminous efficiency depends on the spectral response of the detector. For purely orientation, rather than predictive, purposes, a luminous efficiency of 1% has been assumed in Fig. 1 for the visual region of the spectrum in an attempt to gain insight into the magnitude of the luminous phenomena that might be associated with the collision. The brightness is expressed in apparent vi-

sual stellar magnitudes, that is, as seen from the Earth. It is recalled that the magnitude of the full moon is about  $-12.7$  and that of Jupiter at opposition is  $-2.6$ .

Even if the above estimates are several stellar magnitudes in error, impacts of the largest fragments would generate a spectacular show for an observer located at the right place at the right time. The atmospheric flight of the fragments (at least of some of them) may be observable with the camera on board the Galileo spacecraft. On the other hand, terrestrial observers will apparently not witness the actual explosions (3). Nevertheless, the terminal flares will act as intense flashes of light that for 1 second or less will brightly illuminate the surrounding volume of space, including any of the appropriately located satellites and possibly a section of the ring, and we may be able to detect secondary phenomena triggered by these explosions. Indeed, on the above assumptions, the terminal flare of a penetrating object of an initial mass of  $10^{16}$  g is expected to yield, in the visual passband, a spectral illuminance at a distance of a  $10^6$  km from Jupiter that is six to seven times greater than that of the sun. There is therefore a reasonable chance that evidence will for the first time be gathered on a comet's collision with a planet. Fireball activity on Jupiter was searched for before, but only a single event has ever been recorded (during Voyager 1's encounter in 1979) and investigated (19).

Finally, a caveat is in order. Because there is no known precedent to the expected impact phenomena, considerable uncertainties are necessarily inherent in all the predicted circumstances of this event. The role of the volatile fraction of the comet's fragments (which, unaccounted for in the present calculations, probably further accelerates each object's disintegration process during its atmospheric flight), their interaction with the planet's magnetosphere, their highly uncertain initial (preatmospheric) masses, and uncertainties and variations in their intrinsic ablation rate, material strength, and bulk density, as well as other involved variables, are bound to make the impact phenomena more complicated than is indicated by the predictions based on the model used here. In particular, it is likely that the comet's fragments will experience multiple major outbursts during their flight through the Jovian atmosphere (a behavior that is quite common among the fireballs of class III, especially IIIb, that strike the Earth's atmosphere), in which case their terminal flares could be significantly less prominent than predicted. It therefore is appropriate to emphasize that the results of this investigation should primarily be viewed as descriptions of potential phenomena that can reasonably be expected to take

**Fig. 1.** Energy dissipation curves for objects of various initial masses entering the Jovian atmosphere with a velocity of 59 km/s along a flight path whose minimum distance from the center of Jupiter is  $0.5 R_J$ . Solid curves refer to a cylindrical model for nonrigid objects, and broken curves refer to a less realistic spherical model for rigid projectiles. An apparent visual magnitude that is equivalent to the ablation rate at an assumed 1% luminous efficiency is calculated for Jupiter's geocentric distance of 5.21 astronomical units on 21 July 1994, the time of its anticipated collision with fragments of periodic comet Shoemaker-Levy 9. The character of the peak is strikingly different for the two kinds of projectile in terms of both its appearance and relative position on the curve. The unusually sharp peak for nonrigid objects  $10^4$  g in mass is an artifact of the model, in that the dynamic pressure had surpassed the projectile's material strength shortly before the residual mass reached the terminal point.



place on the assumptions that are the applied model's essential prerequisites. If enough information is gathered in July 1994 from observations of the unprecedented event so that our understanding of the processes involved in a hypervelocity collision between Jupiter and a comet is greatly improved, I will be quite satisfied if this investigation is helpful in contributing incentives that stimulate such a worthy observational campaign.

## REFERENCES AND NOTES

1. C. S. Shoemaker *et al.*, *IAU Circ. No. 5725* (1993); D. H. Levy, *Sky Telesc.* **86**, 38 (1993).
2. J. Luu and D. Jewitt, *IAU Circ. No. 5730* (1993); J. V. Scotti, *IAU Circ. Nos. 5725 and 5745* (1993).
3. S. Nakano, *IAU Circ. No. 5800* (1993); *Minor Planet Circ. No. 22031* (1993); D. K. Yeomans and P. Chodas, *Minor Planet Circ. No. 22197* (1993); *JPL Interoffice Memo. 314.10-50* (1993); personal communication.
4. E. E. Barnard, *Astron. Nachr.* **122**, 267 (1889); *ibid.* **125**, 177 (1890).
5. Z. Sekanina, *Icarus* **30**, 574 (1977); *ibid.* **33**, 173 (1978).
6. \_\_\_\_\_ and D. K. Yeomans, *Astron. J.* **90**, 2335 (1985).
7. H. R. Aggarwal and V. R. Oberbeck, *Astrophys. J.* **191**, 577 (1974). The issue of tidal fracture was also addressed by P. D. Noerdlinger [*Bull. Am. Astron. Soc.* **12**, 829 (1980)] and some of its aspects were further developed by A. R. Dobrovolskis [*Icarus* **88**, 24 (1990)].
8. H. A. Weaver *et al.*, in preparation.
9. G. S. Orton, "Atmospheric Structure in the Equatorial Region of Jupiter," a report of the Galileo Working Group on Atmospheres, Subcommittee on Atmospheric Structure (1981), pp. 9-13.
10. G. F. Lindal *et al.*, *J. Geophys. Res.* **86**, 8721 (1981).
11. C. F. Chyba *et al.*, *Nature* **361**, 40 (1993). Other models and approaches that account for the fragmentation of fireballs have likewise been proposed: for example, B. Baldwin and Y. Sheaffer, *J. Geophys. Res.* **76**, 4653 (1971); and J. G. Hills and M. P. Goda, *Astron. J.* **105**, 1114 (1993). For applications of a gross-fragmentation approach to photographic data on fireballs, see Z. Ceplecha and R. E. McCrosky, in *Asteroids, Comets, Meteors 1991*, A. W. Harris and E. Bowell, Eds. (Lunar and Planetary Institute, Houston, TX, 1992), pp. 109-112; and Z. Ceplecha, in *Meteoroids and Their Parent Bodies*, J. Štohl and I. P. Williams, Eds. (Slovak Academy of Sciences, Bratislava, Slovakia, 1992), pp. 287-294.
12. Z. Ceplecha, *Bull. Astron. Inst. Czech.* **28**, 328 (1977). For similar recommended values of  $\rho$  and  $\sigma$ , see D. O. ReVelle, *Meteoritics* **18**, 386 (1983); Z. Ceplecha, *Publ. Astron. Inst. Czech. Acad. Sci. No. 67* (1987), pp. 211-215; *Bull. Astron. Inst. Czech.* **39**, 221 (1988). For the introduction of the fireball classification, see Z. Ceplecha and R. E. McCrosky, *J. Geophys. Res.* **81**, 6257 (1976). ReVelle remarks that for cometary objects penetrating the Jovian atmosphere, one may expect an ablation coefficient that is even higher than  $0.2 \text{ s}^2/\text{km}^2$ . Aerodynamic effects and flow phenomena during a flight through the Jovian atmosphere were investigated primarily for the purpose of optimizing the configuration of an entry probe to be delivered by a Jupiter-bound mission [G. D. Walberg *et al.*, *Acta Astronautica* **4**, 555 (1977); S. N. Tiwari and S. V. Subramanian, *ibid.* **7**, 583 (1980); and a number of references quoted therein], and the results are not directly applicable to a collision with a comet fragment.
13. Z. Sekanina, *Astron. J.* **90**, 827 (1985).
14. At least two such events were observed and documented in the Earth's atmosphere; see L. G. Jacchia, *Sky Telesc.* **48**, 4 (1974); Z. Ceplecha, *Bull. Astron. Inst. Czech.* **30**, 349 (1979); and J. Borovička and Z. Ceplecha, *Astron. Astrophys.* **257**, 323 (1992).
15. D. D. Laumbach and R. F. Probst, *J. Fluid Mech.* **35** (part 1), 53 (1969); *ibid.* **40** (part 4), 833 (1970); V. P. Korobeinikov, *Annu. Rev. Fluid Mech.* **3**, 317 (1971); *Problems in the Theory of Point Explosions in Gases* (American Mathematical Society, Providence, RI, 1976).
16. Z. Sekanina, *Astron. J.* **88**, 1382 (1983). The fireball light curves shown are smoothed tabulated data from the Prairie Network, operated by R. E. McCrosky and colleagues, and from the European Network, operated by Z. Ceplecha and his co-workers.
17. Z. Ceplecha, in *Solid Particles in the Solar System*, I. Halliday and B. A. McIntosh, Eds. (Reidel, Dordrecht, Netherlands, 1980), pp. 171-183. Comparison of D. O. ReVelle's and V. Padevél's ablation models shows discrepancies in the luminous efficiencies from about one order of magnitude for type I fireballs up to about three orders of magnitude for type IIIb fireballs.
18. For especially elucidating discussions of the luminous efficiencies of the three photographed fireballs that produced the known meteorites, see Z. Ceplecha, *Bull. Astron. Inst. Czech.* **12**, 21 (1961); R. E. McCrosky, A. Posen, G. Schwartz, C.-Y. Shao, *J. Geophys. Res.* **76**, 4090 (1971); D. O. ReVelle and R. S. Rajan, *ibid.* **84**, 6255 (1979); and I. Halliday, A. A. Griffin, A. T. Blackwell, *Meteoritics* **16**, 153 (1981). Also important are relevant laboratory simulations and studies of artificial meteors: W. G. Ayers, R. E. McCrosky, C.-Y. Shao, *SAO Spec. Rep. No. 317* (Smithsonian Astrophysical Observatory, Cambridge, MA, 1970); J. J. Givens and W. A. Page, *J. Geophys. Res.* **76**, 1039 (1971); J. F. Friich-tenicht and D. G. Becker, in "Evolutionary and Physical Properties of Meteoroids," NASA SP-319, C. L. Hemenway, P. M. Millman, A. F. Cook, Eds. (1973), pp. 53-81.
19. A. F. Cook and T. C. Duxbury, *J. Geophys. Res.* **86**, 8815 (1981).
20. Investigators interested in a detailed tabulation of variations in the physical parameters of the model objects during their flight through the Jovian atmosphere may obtain the pertinent computer files upon request. Separately for each of the two models, the files list for each assumed initial projectile mass the following quantities at some 25 to 50 points along the trajectory between an initial reference height of 1000 km above 1-bar pressure level and a terminal height (or a height of 1000 km outbound for surviving objects): time (reckoned from the initial point), height, atmospheric pressure, atmospheric density, the projectile's residual mass, its frontal area (for the nonrigid objects only), its velocity and acceleration (sum of  $V_{\text{drag}}$  and  $V_{\text{grav}}$ ), aerodynamic pressure, energy dissipation rate per unit time and per unit height, and cumulative dissipated energy.
21. I thank G. S. Orton for making his atmospheric model of Jupiter available for this investigation, and P. Chodas, D. K. Yeomans, and B. G. Marsden for keeping me updated on the progress in the ongoing orbit-determination efforts. I benefited from comments on a draft of this paper by Z. Ceplecha, E. Grun, I. Halliday, and D. O. ReVelle. I am also grateful for constructive critiques by M. F. A'Hearn and an anonymous referee. This research was carried out by the Jet Propulsion Laboratory, California Institute of Technology, under contract with the National Aeronautics and Space Administration.

## RESEARCH ARTICLES

# Human CksHs2 Atomic Structure: A Role for Its Hexameric Assembly in Cell Cycle Control

Hans E. Parge, Andrew S. Arvai, Darren J. Murtari, Steven I. Reed, John A. Tainer\*

The cell cycle regulatory protein CksHs2 binds to the catalytic subunit of the cyclin-dependent kinases (Cdk's) and is essential for their biological function. The crystal structure of the protein was determined at 2.1 Å resolution. The CksHs2 structure is an unexpected hexamer formed by the symmetric assembly of three interlocked dimers into an unusual 12-stranded  $\beta$  barrel fold that may represent a prototype for this class of protein structures. Sequence-conserved regions form the unusual  $\beta$  strand exchange between the subunits of the dimer, and the metal and anion binding sites associated with the hexamer assembly. The two other sequence-conserved regions line a 12 Å diameter tunnel through the  $\beta$  barrel and form the six exposed, charged helix pairs. Six kinase subunits can be modeled to bind the assembled hexamer without collision, and therefore this CksHs2 hexamer may participate in cell cycle control by acting as the hub for Cdk multimerization *in vivo*.

Cell cycle progression in eukaryotes is regulated at two principal transition points, one that occurs before DNA replication (1) and the other that occurs before mitosis

(2). Both transitions are controlled by the activation of specialized essential protein kinases called cyclin-dependent kinases or Cdk's (3, 4). Cdk catalytic subunits alone